

P.311 Multiple Doppler Radar Analysis of External Environmental and Topographical Influences on a QLCS Tornado Event

Anthony W. Lyza¹, Ryan A. Wade, Todd A. Murphy, Timothy A. Coleman, and Kevin R. Knupp
Severe Weather Institute-Radar and Lightning Laboratories (SWIRLL)

University of Alabama in Huntsville, Huntsville, AL

1. Introduction

On 11 April 2013, a localized severe weather episode evolved across Mississippi, Alabama, and Georgia, producing several tornadoes, along with incidences of wind damage. Two of these tornadoes impacted Redstone Arsenal and the south side of the city of Huntsville, Alabama, during the early rush hour period, between 2120 UTC and 2134 UTC. These tornadoes, both rated EF1 on the Enhanced Fujita Scale, produced damage to trees, power lines, homes, and other structures (NWS Huntsville 2013; hereafter NWS; Fig. 1).

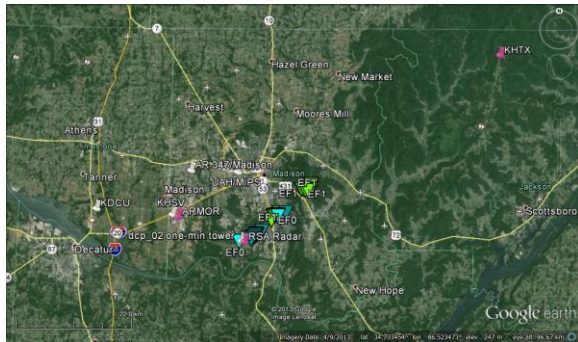


Fig. 1: Overview map for 11 April 2013, containing the locations of the Huntsville (KHSV) and Decatur (KDCU) ASOS sites, the WSR-88D radar at Hytop, AL (KHTX), the Advanced Radar for Meteorological and Observations research (ARMOR), the Redstone Arsenal S-band Doppler radar (RSA Radar), and the location of the UAH surface station and Mobile Integrated Profiling System (UAH/MIPS). National Weather Service Huntsville survey points for the 11 April 2013 tornadoes are indicated by the blue and green triangles. Image produced on Google Earth.

¹Corresponding author address:

Anthony W. Lyza
Department of Atmospheric Science, University of
Alabama in Huntsville
320 Sparkman Dr.
Huntsville, AL 35805
Email: lyzaa@nsstc.uah.edu

Numerous studies have been undertaken regarding the dynamics of tornadoes spawned by quasi-linear convective systems (QLCSs) and their associated mesovortices. This event, however, features unique behaviors and interactions between the mesovortex and features both external and internal to the QLCS that warrant close examination. The first and foremost of these behaviors is the interaction between the tornado/mesovortex and the terrain on the south side of Huntsville. Significant changes in the motion, intensity, and structure of the mesovortex and attendant tornado circulation were observed in the vicinity of Huntsville Mountain, which bisected the two identified tornado damage tracks. An additional unique feature observed is a gust front to the north of the tornadic mesovortex that was associated with a pressure *drop* at multiple observing sites. A decaying bookend vortex that was a result of a supercell merger with the QLCS was also present in the vicinity of the mesovortex and the atypical gust front, and may have played a significant role in the evolution of these features.

These features all evolved within a high-resolution array of in-situ and ground-based remote sensing platforms in north-central Alabama (Fig. 1). These platforms will be further discussed in Section 2. The motivation for this study is to serve as an impetus toward a quantified analysis of the observed effects of topography on deep convection-produced circulations, including mesocyclones, QLCS mesovortices, and tornadoes. This case provides an excellent example of the latter two features interacting with significant topography within a high-resolution observation array. Additional motivation for this study is provided by the unique gust front structure profiled by vertically-pointed instruments and multiple surface observation sites within the data array. Details regarding the collection of the data within this array and the methodology of the analysis are given in section 2.

2. Data Collection and Methodology

As mentioned in Section 1, the unique evolution of the 11 April 2013 QLCS occurred within a remarkably high-resolution observational domain. These in-situ and ground-based remote sensing platforms include the C-band Advanced Radar for Meteorological and Observational Research (ARMOR), the Mobile

Alabama X-band radar (MAX), the Weather Surveillance Radar-88 Doppler (WSR-88D) located at Hytop, Alabama, (KHTX), the S-band Doppler radar located at Redstone Arsenal (RSA radar), the Mobile Integrated Profiling System (MIPS), which features a vertically-pointed X-band radar (XPR), a 915-MHz Doppler wind profiler, a 12-channel microwave profiling radiometer (MPR), and a lidar ceilometer, the Huntsville (KHSV) and Decatur (KDCU) Automatic Surface Observing Station (ASOS) sites, a 5-second resolution surface observing site at the University of Alabama in Huntsville (UAH), and a one-minute resolution observing site located at the southeast end of Redstone Arsenal (dcp02). All of these observation platforms were fully functional on 11 April 2013 with the exception of the RSA radar, which suffered a power outage at approximately 2118 UTC, just prior to the first tornadogenesis event.

For the purposes of this paper, data from ARMOR, UAH, MIPS, KHTX, and dcp02 are highlighted in the examination of the tornadic mesovortex and other pertinent features previously mentioned. ARMOR was operating in a three-tilt RAIN-1 scheme, providing data from 0.7° , 1.3° , and 2.0° tilts with a completion time of 66 to 69 seconds per complete RAIN-1 scan, for the entire study period except for the period between 2112 UTC and 2116 UTC, when a 6-tilt partial volume up to 5.1° was completed. The close range of ARMOR to the mesovortex and tornado, in conjunction with its rapid low-level scans, provided an excellent low-level dataset for the evolution of the mesovortex and a more in-depth single-Doppler analysis (Section 3). The dcp02 surface station on Redstone Arsenal was directly impacted by the developing mesovortex immediately prior to tornadogenesis (as estimated from NWS damage assessment and ARMOR TDS detection) and will also be examined. Additionally, the UAH surface site and MIPS were directly impacted by the gust front and the decaying mesovortex, which provided a spectacular vertical profiling dataset that will be analyzed in section 4.

3. Mesovortex Evolution

The mesovortex that produced the Huntsville tornadoes was first detected on ARMOR radar at 2112 UTC and began to rapidly intensify as the QLCS propagated to the northeast. Figure 2 shows a cross-section of the leading edge of the QLCS as view from KHTX at 2116 UTC, with a clearly identifiable descending rear-inflow jet (Weisman 1992 and others), which past studies have shown to play a significant role in mesovortex formation and intensification (Trapp and Weisman 2003 and others). Figure 4 shows the dcp02

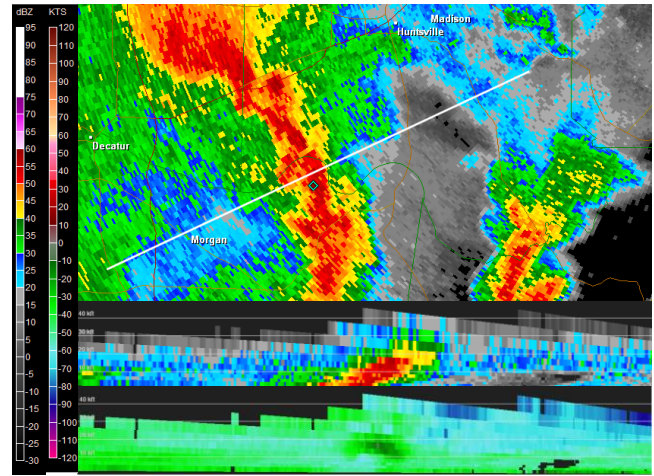


Fig. 2: 2116 UTC base reflectivity PPI (top), cross-section (middle), and base velocity cross-section (bottom) from KHTX radar.

observation trace from Redstone Arsenal, very near where the first tornado formed. A substantial backing of the winds was observed ahead of the mesovortex, with the direction reaching 52° begin to veer as the mesovortex passed. A peak gust of 24 m s^{-1} (47 kt) was observed at 2121 UTC. A steady pressure drop was also noted ahead of the mesovortex, with a rapid rise immediately following the mesovortex with the passage of the gust front.

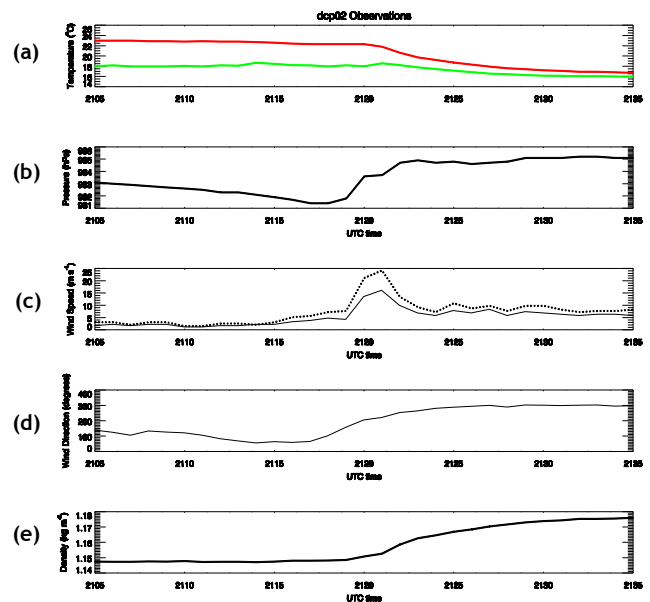


Fig. 3: 1-min. resolution data from Redstone observation site dcp02 of a) 2-m temperature ($^\circ\text{C}$; red) with 2-m dewpoint ($^\circ\text{C}$; green); b) 2-m pressure (hPa), c) 2-m wind speed (m s^{-1} ; solid) and peak gust (m s^{-1} ; dashed), d) 2-m wind direction (degrees), and e) 2-m density (kg m^{-3}).

Tornadogenesis of the first tornado (hereafter the “Lily Flagg Rd. tornado”) was estimated at 2120 UTC based off of an observed tornado debris signature (TDS; Ryzhkov et al. 2005, Schultz et al. 2012; Figure 4) from the ARMOR radar. In addition to the TDS, a prominent curl in reflectivity and a Z_{DR} arc/curl were observed. The survey from NWS Huntsville indicates EF1 damage with peak winds estimated at approximately 40 m s^{-1} (90 MPH). The lead author conducted an independent damage survey and reached the same conclusion. The TDS was present until 2128 UTC.

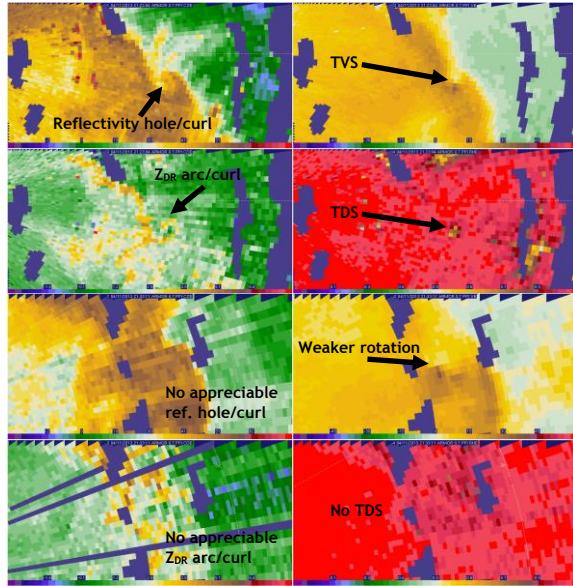


Fig. 4: Four-panel plots of corrected reflectivity (dBZ; upper-left), dealiased base velocity (m s^{-1} ; upper-right), corrected differential reflectivity (dB; lower-left) and correlation coefficient (lower-right) at 0.7° from ARMOR at 21:23:04 UTC (top) and 21:33:11 UTC (bottom), at about the respective times of peak intensity for the Lily Flagg Rd. and Dug Hill Rd. tornadoes.

After the initial tornado dissipated, the mesovortex crossed Huntsville Mountain, an elevation rise of approximately 260-280 meters above the surrounding terrain. Upon descending Huntsville Mountain, the second tornado (hereafter the “Dug Hill Rd. tornado”) formed at approximately 2132 UTC. As seen in Figure 4, the Dug Hill Rd. tornado was not accompanied by a TDS, nor was it associated with a notable curl in reflectivity or a Z_{DR} arc/curl. Despite the lack of notable ARMOR observations, damage from both the NWS and lead author’s surveys indicated more intense damage, with winds estimated around 47 m s^{-1} (105 MPH).

Further analysis was performed on the ARMOR single-Doppler data to diagnose the changes in the mesovortex as it interacted with Huntsville Mountain. The location of the mesovortex in the observational

array was somewhat unfortunate in that it was in the ARMOR-KHTX baseline for dual-Doppler analysis, and the distance from the MAX site coupled with precipitation falling over MAX led to significant signal loss immediately behind the convective line, making a dual-Doppler synthesis of the mesovortex during the tornadic lifetime a futile exercise. Additionally, the very rapidly-evolving nature of the mesovortex eliminated the employment of a synthetic or pseudo-dual-Doppler technique. Nonetheless, an in-depth single Doppler analysis of ARMOR data was able to be performed at high low-level temporal resolution, owing to the previously-mentioned 3-tilt RAIN-1 scans. A Rankine-combined vortex was used similar to Brown and Wood (1991), assuming a circular, axisymmetric vortex, to estimate rotational velocity, axisymmetric vertical vorticity, and axisymmetric divergence within the circulation. A similar treatment of single-Doppler radar data of a tornado vortex can be found in Alexander and Wurman (2005). Once the circulation center was estimated, the center point was entered into Google Earth to estimate the land surface elevation under the vortex. Figure 5 shows the results of this analysis, giving a time-height section of the computed rotational velocity, axisymmetric vertical vorticity, and axisymmetric divergence values, along with a time-height section of the land surface elevation directly underneath the mesovortex. Figure 6 is a Google-Earth generated map of the estimated circulation center locations overlaid a satellite view of the surface.

The rotational velocity and axisymmetric vertical vorticity analyses show a very distinct maximum in both values during the lifespan of the Lily Flagg Rd. tornado. The values of rotational velocity generally range from $16\text{-}18 \text{ m s}^{-1}$, while the axisymmetric vertical vorticity values range from $4\text{-}8 \times 10^{-2} \text{ s}^{-1}$. These values quickly diminish as the mesovortex begins to cross Huntsville Mountain, reaching a relative minimum almost directly over the mountain (note that the mountain peak was filled in in the analysis using the segment between the two nearest analyzed center points as the circulation center was never directly overtop the mountain peak). Upon descending Huntsville Mountain, a slight increase in both rotational velocity and axisymmetric vertical vorticity are noted, with values of rotational velocity generally near $14\text{-}16 \text{ m s}^{-1}$ and axisymmetric vertical vorticity values of approximately $2\text{-}4 \times 10^{-2} \text{ s}^{-1}$. Additionally, convergence peaks prior to tornadogenesis of the Lily Flagg Rd. tornado, but does not exhibit such a peak prior to the genesis of the Dug Hill Rd. tornado. The implications of these results are discussed in Section 5.

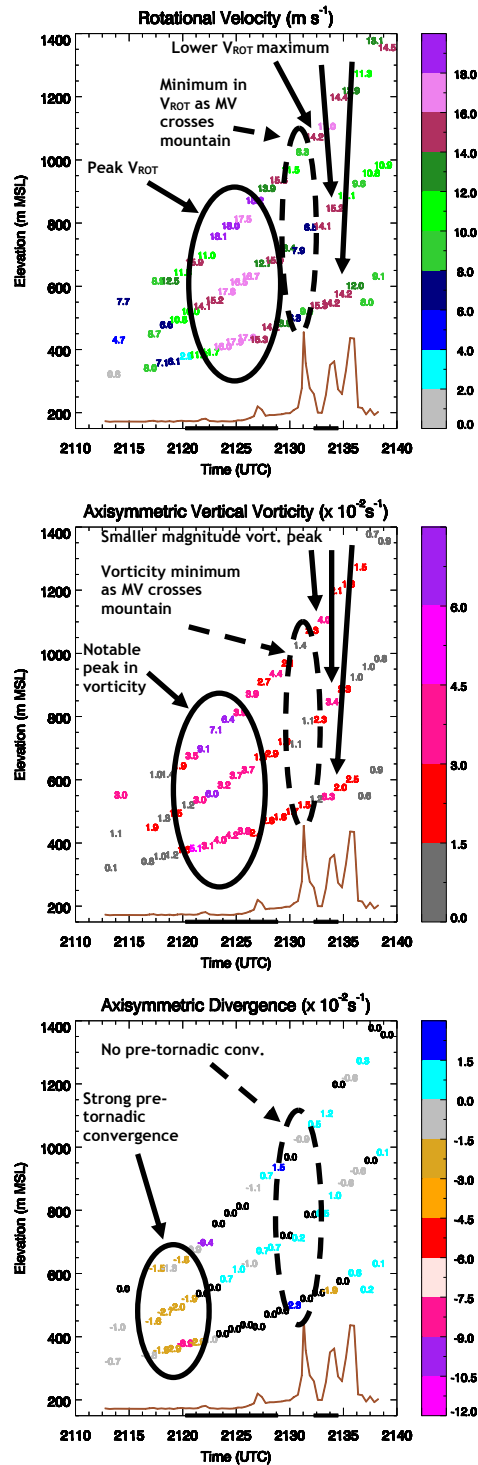


Fig. 5: Rotational velocity (V_{ROT} ; top), axisymmetric vertical vorticity (middle) and axisymmetric divergence (bottom) of the Huntsville tornadic mesovortex (MV) from 2116-2136 UTC 11 April 2013, as estimated from ARMOR data. The brown line indicates land surface elevation underneath the center of the mesovortex at each time indicated, and the bold black lines along the time axis indicate the Storm Data times of tornado occurrence.

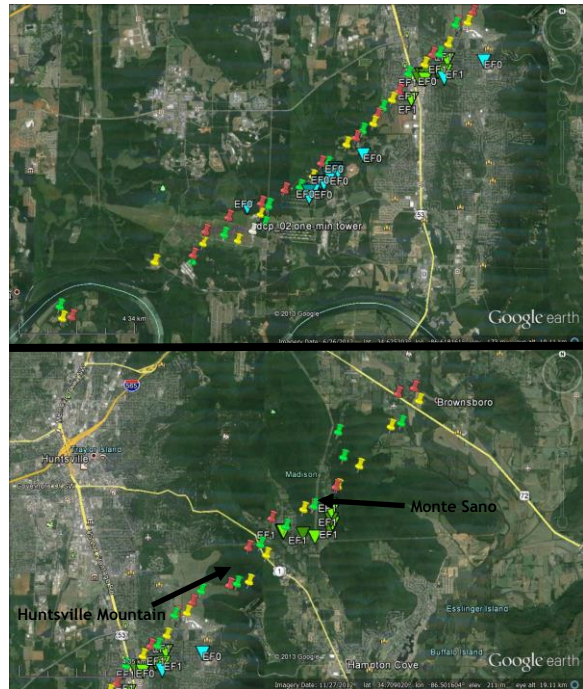


Fig. 6: Zoomed-in view of the Lily Flagg Rd. (top) and Dug Hill Rd. (bottom) tornado tracks as surveyed by NWS Huntsville (triangles), and the center-points of the mesovortex as estimated by ARMOR (green = 0.7° , yellow = 1.3° , red = 2.0°).

4. The Gust Front and Decaying Bookend Vortex

The gust front associated with the 11 April 2013 QLCS first impacted the UAH/MIPS location at approximately 2114 UTC. The surface trace from UAH is shown in Figure 7. The pressure and temperature traces are particularly notable. Note that the temperature drop is immediately accompanied by a pressure drop. From 21:14:40 UTC to 21:22:00 UTC, the pressure drops 1.25 hPa, from 979.27 hPa to 978.02 hPa. Immediately following the pressure drop, a rapid pressure rise was observed, with pressure rising from 978.02 hPa to 981.27 hPa (3.25 hPa) between 21:22:40 UTC and 21:27:00 UTC, with much of that pressure rise commencing at around 2124 UTC. As seen in the time-height cross-sections from the XPR in Figure 8, the rapid rise in pressure appeared to coincide with the passage of the decaying bookend vortex and associated strong updraft region. Figure 8 shows a profile of the gust front sampled by the XPR on the MIPS platform. From the XPR, the depth of the density current is estimated at approximately 800 m. The propagation speed as estimated from ARMOR was approximately 12.5 m s^{-1} . The peak 5-second wind gust at UAH was 13.74 m s^{-1} at 21:23:10 UTC, only about 30 seconds after the pressure minimum was reached and about 50

seconds before the rise in pressure fully commenced. These results are further discussed in Section 5.

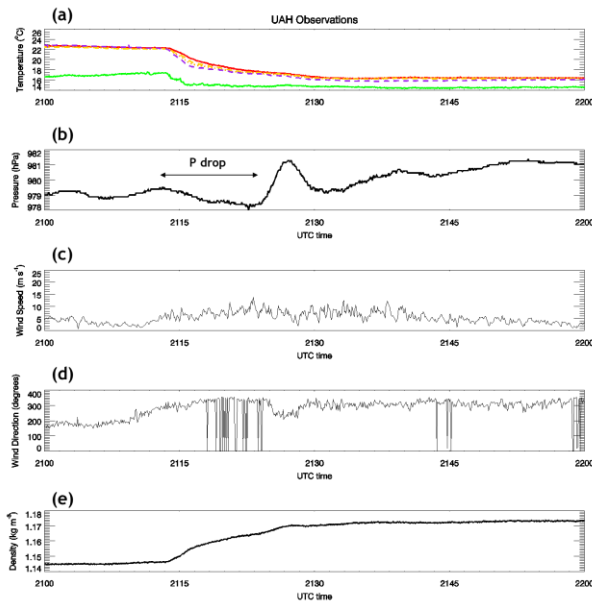


Fig. 7: 5-sec. resolution data from UAH observation site of a) 0.5-m (gold), 1.0-m (orange), 2-m (red), and 10-m (purple) temperatures ($^{\circ}\text{C}$) with 2-m dewpoint ($^{\circ}\text{C}$; green); b) 2-m pressure (hPa), c) 10-m wind speed (m s^{-1}), d) 10-m wind direction (degrees), and e) 2-m density (kg m^{-3}).

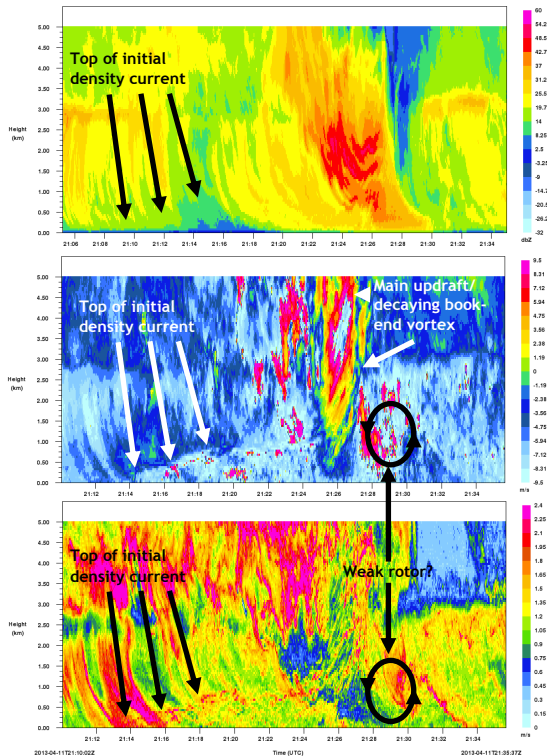


Fig. 8: Uncorrected equivalent reflectivity (Z_e), particle vertical velocity (W), and spectrum width time-height cross-sections from the X-band, vertically-pointed radar (XPR) for 0-5 km depth, 2110-2135 UTC 11 April 2013. Nyquist velocity is 9.5 m s^{-1} .

5. Summary/Future Work

The 11 April 2013 Huntsville, AL QLCS event provided a variety of unique observations of a squall line and an associated tornadic mesovortex. It provided an opportunity for high-resolution, low-level radar data on a profound mesovortex/terrain interaction, as well as high-resolution vertical profiling data of a gust front structure featuring a rare surface temperature/pressure pattern.

The data on the tornadic mesovortex are particularly compelling. Even though the second of the two tornadoes was observed to have produced more significant damage, the parent mesovortex was associated with merely half of the magnitude of vorticity observed while the first tornado was in progress. This observation lends credence to the idea that the restrengthening of the tornadic circulation was relegated to the lowest levels of the atmosphere within the surface layer. One potential explanation for this intensification may be corner flow collapse (Lewellen and Lewellen 2007), which has been shown in preliminary modeling studies to potentially lead to the rapid near-surface intensification of a tornadic vortex as it descends a mountain (Lewellen 2012). Furthermore, there is a possibility that this occurred twice in the lifespan of the mesovortex, as the second tornado crossed the southeastern tip of Monte Sano (second elevation peak in Figure 5). It should be noted that it was assumed in the damage survey process, since sporadic damage was observed all along Dug Hill Rd., that the second tornado was continuous, although more significant damage was once again observed after the tornado descended Monte Sano (lead author's survey).

An additional note must be made of the structure and motion of the mesovortex. The coherence of the structure is inferred from the pattern of the center points in Figure 6. During the Lily Flagg Rd. tornado, the mesovortex is quite coherent, with the center points lining up in a nearly straight line and very near the observed tornado damage. However, as the mesovortex approaches Huntsville Mountain, it becomes less coherent, stalls, move into a gap, and then jumps or reforms across the peak of the mountain. Lewellen (2012) does briefly mention jumping/reforming of vortices occurring in his modeling studies. Future work should make further analysis of these phenomena, including rigorous documentation in surveys as well as large-eddy simulation modeling as in Lewellen (2012), a priority.

The gust front profile observed by UAH/MIPS also raise intriguing questions. Surprisingly, when using the formula to estimate a pressure perturbation associated with a gust front (derived from Markowski and Richardson 2010, keeping the pressure perturbation term):

$$p'(H) = p_0(0.5c^2 - gH((\rho_2 - \rho_1)/\rho_1)) \quad (1)$$

where:

$p'(H)$ = perturbation pressure as a function of density current depth

p_0 = a background density

c = propagation speed of the density current

$g = 9.81 \text{ m s}^{-2}$

H = depth of the density current

ρ_1 = density within the density current

ρ_2 = density outside the density current

and using the values observed and described in Section 4, a pressure perturbation of -0.654 hPa is predicted, which, while not quite the -1.25 hPa observed, does show that the negative pressure perturbation can be predicted theoretically in this case. Further analysis of this event will include an in-depth analysis of the potential role that the decaying bookend vortex had in the evolution of the gust front.

Additional future work will include expanding a database of tornado events potentially affected by topography. It is only through such a database that quantified relationships between topography and tornado, mesocyclone, and mesovortex evolution will begin to shed more light on these fascinating interactions.

References

- Alexander, Curtis R., Joshua Wurman, 2005: The 30 May 1998 Spencer, South Dakota, Storm. Part I: The Structural Evolution and Environment of the Tornadoes. *Mon. Wea. Rev.*, **133**, 72–97.
- Brown, Rodger A., Vincent T. Wood, 1991: On the Interpretation of Single-Doppler Velocity Patterns within Severe Thunderstorms. *Wea. Forecasting*, **6**, 32–48.
- Lewellen, D. C., W. S. Lewellen, 2007: Near-Surface Vortex Intensification through Corner Flow Collapse. *J. Atmos. Sci.*, **64**, 2195–2209.
- Lewellen, D. C., 2012: Effects of Topography on Tornado Dynamics: A Simulation Study. Preprints, *26th Conference on Severe Local Storms*, Nashville, TN, Amer. Meteor. Soc.
- Markowski, P., and Y. Richardson, 2010: Density current dynamics. *Mesoscale Meteorology in Midlatitudes*, Wiley-Blackwell, 142–149.
- National Weather Service, Huntsville, AL, 2013: *Severe Weather Event on April 11, 2013*. <http://www.srh.noaa.gov/hun/?n=hun_sur_2013-04-11>
- Ryzhkov, Alexander V., Terry J. Schuur, Donald W. Burgess, Dusan S. Zrnic, 2005: Polarimetric Tornado Detection. *J. Appl. Meteor.*, **44**, 557–570.
- Schultz, C.J., L.D. Carey, E.V. Schultz, B.C. Carcione, C.B. Darden, C.C. Crowe, P.N. Gatlin, D.J. Nadler, W.A. Petersen, and K.R. Knupp, 2012: Dual-Polarization Tornadic Debris Signatures Part I: Examples and Utility in an Operational Setting. *Electronic J. Operational Meteor.*, **13** (9), 120–137.
- Trapp, Robert J., Morris L. Weisman, 2003: Low-Level Mesovortices within Squall Lines and Bow Echoes. Part II: Their Genesis and Implications. *Mon. Wea. Rev.*, **131**, 2804–2823.
- Weisman, Morris L., 1992: The Role of Convectively Generated Rear-Inflow Jets in the Evolution of Long-Lived Mesoconvective Systems. *J. Atmos. Sci.*, **49**, 1826–1847.